Implementation of an Autoregressive Wave Model in a Numerical Simulation Code

Kenneth Weems, Arthur M. Reed
(David Taylor Model Basin, Carderock Division, Naval Surface Warfare Center),
Alexander B. Degtyarev, Ivan Gankevich
(St. Petersburg State University)

ABSTRACT

An autoregressive wave model is described and its implementation in a time-domain numerical simulations of ship motions and loads in irregular waves is discussed.

An important part of applying an autoregressive wave model is the calculation of the 3-D velocity potential field for an incident wave described only by the shape of the free surface. Most time domain seakeeping simulation codes require the pressure and velocity of the incident wave over the ship's hull surface or the boundaries of the computational domain, but non-traditional wave models, including the ARM, only provide the shape of the free surface. This paper describes a highly efficient procedure for computing the velocity potential field beneath a prescribed nonlinear wave surface.

INTRODUCTION

A key element of any assessment of the motions or loads of a ship or marine vehicle in ocean waves is a model of the incident, wind-driven seaway, which must provide a physically realistic representation of the wave surface and the stochastic properties of "random" ocean waves. For many numerical simulations, the model must also include the corresponding velocity field and pressure beneath the surface. The most popular model is that of Longuet-Higgins (1962), which is based on a stochastic approximation of the moving wave-front as a superposition of elementary harmonic waves with random phases and random amplitudes: ε_n, c_n, respectively:

$$\zeta(x,y,t) = \sum_n c_n \cos(u_n x + v_n y - \omega_n t + \varepsilon_n) \qquad (1)$$

The vector wave number (u_n, v_n) is continuously distributed on the (uv)-plane and is related to the frequency ω_n by a deterministic dispersion relation. The phase angles ε_n are jointly independent random variables uniformly distributed in the interval $[0, 2\pi]$.

Longuet-Higgins showed that under the above conditions, the function $\zeta(x,y,t)$ is a three-dimensional steady-state homogeneous ergodic Gaussian field, defined by

$$2E_\zeta(u,v)\,du\,dv = \sum_n c_n^2 \qquad (2)$$

where $E_\zeta(u,v)$ is the two dimensional spectral density of wave energy.

Longuet-Higgins' model is simple and is easily computed. It incorporates the physical fundamentals of the process of wind waves and is fully consistent with the task of modeling ocean waves.

Importantly, at least for the purposes of numerical simulation, an explicit expression for the corresponding 3-D velocity potential can be derived by linearizing the free surface boundary condition, resulting in the well known formula for the deep-water wave potential:

$$\begin{aligned}\phi(x,y,z,t) = \sum_n \frac{c_n g}{\omega_n} e^{(\sqrt{u_n^2+v_n^2}z)} \\ \times \sin(u_n x + v_n y - \omega_n t + \varepsilon_n)\end{aligned} \qquad (3)$$

This formula can be analytically differentiated to provide the incident wave velocity field and pressure, and is readily integrated into both linear and nonlinear (via Wheeler stretching) numerical simulation codes. Thus, Longuet-Higgins' model is distinguished by its considerable clarity and the simplicity of the computational algorithm. However, it is not without some serious shortcomings inherent in models of this class:

- The Longuet-Higgins' model is only designed to represent a stationary Gaussian field. Normal distribution of the simulated process is a consequence of the central limit theorem. Its application to the analysis of more general problems such as the evolution of ocean waves in a storm, or the study of

ocean waves distorted by shallow water represents a significant challenge.

- Models of this class are periodic and need a very large number of frequencies in order to generate statistically independent non-repeating waves for long simulations (Belenky, 2005) and the computation time increase linearly with the number of frequencies.
- In the numerical implementation of the Longuet-Higgins' model, it appears that the rate of statistical convergence is very slow. This is seen as a distortion of the energy spectrum of the simulated process.
- The Longuet-Higgins model is not obviously appropriate when simulating complex waves that have a broad spectrum with many peaks, and when describing extreme events.

These latter three points become particularly critical in numerical simulation. In a time domain computation of the responses of a vessel in a random seaway, the repeated evaluation of the velocity at hundreds or thousands of points on the hull, for thousands or tens of thousands of time steps can become a major factor, determining the execution speed of the code (Beck & Reed, 2001). This becomes an even more significant issue in a nonlinear computation where the wave model is even more complex. Developing a less time intensive method for modeling the ambient ocean-wave environment has the potential for significantly speeding up the total simulation process.

AN AUTOREGRESSIVE MODEL OF OCEAN WAVES

An autoregressive model (ARM) of ocean waves is an alternative approach that models a stochastic moving surface as a linear transformation of white noise with memory. ARMs are commonly used in other areas of probabilistic mechanics and dynamics to model stationary ergodic Gaussian random processes with given correlation characteristics (Box, *et al.*, 2008), but they have not been applied extensively to wind waves.

One dimensional Wind Wave Model

The formal mathematical framework of regressive wave models was developed by Spanos (1983), Gurgenidze & Trapeznikov (1988) and Rozhkov & Trapeznikov (1990). The latter built a one-dimensional model of ocean waves $\zeta(t)$, on the basis of an autoregressive-moving average (ARMA) model

$$\zeta_t = \sum_{i=1}^{N} \Phi_t \zeta_{t-i} + \sum_{j=0}^{P} \Theta_j \varepsilon_{t-j}. \tag{4}$$

Here Φ_j are the autoregressive parameters, Θ_j the parameters of the moving average, and ε_j the white noise with an infinitely divisible distribution law.

In practice, it has been more common to use an autoregressive model:

$$\zeta_t = \sum_{i=1}^{N} \Phi_t \zeta_{t-i} + \varepsilon_t \tag{5}$$

which can be directly related to the power spectrum of the seaway:

$$S_\zeta(\omega) = \frac{\sigma_\varepsilon^2}{2\pi} \frac{\Delta}{\left|1 + \sum_{j=1}^{N} \Phi_j \exp[-ij\Delta\omega]\right|^2} \tag{6}$$

where ζ_t is the wave elevation at time t, N is the order of the model, Φ_i are the regression coefficients, ζ_{t-i} are the N last realizations of $\zeta_t, [i = 1, \ldots, N]$, ε_t is Gaussian white noise with variance σ_ε^2, and Δ is the sampling interval of the series.

The autoregressive coefficients of (5) can be estimated from the autocovariance function (K_ζ) by solving the Yule-Walker equations:

$$K_\zeta(i) = \sum_{k=0}^{N} \Phi_k K_\zeta(k-i) \tag{7}$$

and the variance of the white noise σ_ε^2 can be calculated as:

$$\sigma_\varepsilon^2 = V_\zeta - \sum_{j=0}^{N} \Phi_j K_\zeta(j) \tag{8}$$

The derivation of these formulae can be found in Degtyarev & Reed (2011).

In theory, the number of autoregressive coefficients N tends to infinity. In practice, it has been found that remarkably few coefficients are required to recreate the wave surface and to recover the stochastic properties of the wave. As the periodicity of the wave evaluation is dependent only on the random number generator, this suggests that very long wave records can be modeled without self-repeat and at very small cost.

To demonstrate this, consider a long-crested (single direction) Fourier series wave model created by discretizing a Bretschneider spectrum for Sea State 6 ($H^{1/3} = 5.0$m, $T_0 = 12.5$s) with 80 wave components as shown in Figure 1.

The relatively low cutoff frequency, which has been selected specifically to maximize the self-repeat time, corresponds to a component wave length of 60 m and is not un-typical of what might be selected for the simulation of a very large ship. Despite this, a plot of the autocovariance of wave elevations computed using this

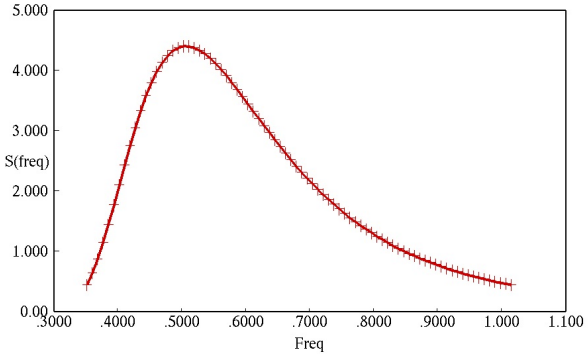

Fig. 1 Typical Spectrum Discretization for Numerical Simulations

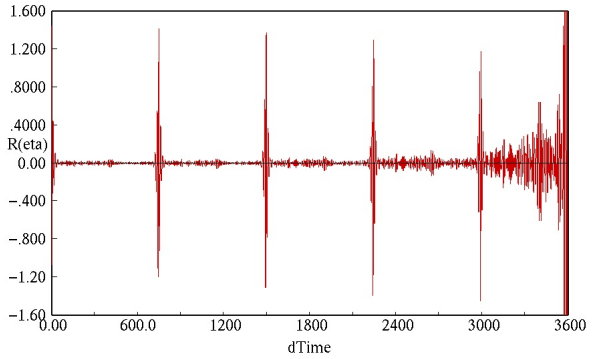

Fig. 2 Auto-covariance for Elevations from Fourier Wave model

wave model (Figure 2) shows a self-repeat time of just 750 s. While there are many tricks that are employed to disrupt this self-repeat, it is clear that a very large number of wave components are required to generate a statistically independent incident Fourier series-based wave model for an irregular sea simulation for any significant length of time (Belenky, 2005).

To create an ARM of waves for this case, the auto-covariance K_ζ can be calculated from a 750 s record of elevation at a point, from which the regression coefficients and variance of white noise can be computed using Equations (7) and (8), respectively. Figure 3 compares the elevations from the Fourier series to elevations from an ARM with a time interment (Δt) of 0.6 s and a regression order (N) of 8. The ARM waves match both quantitatively (variance and distribution) and qualitatively (character of the waves) to the elevation data from which the ARM was derived. As shown in Figure 4, an evaluation of the ARM wave through 25,000 s shows stable elevations and no sign of self-repeat in the auto-covariance function. The elevation evaluation with this low order model is far faster than the Fourier series approach.

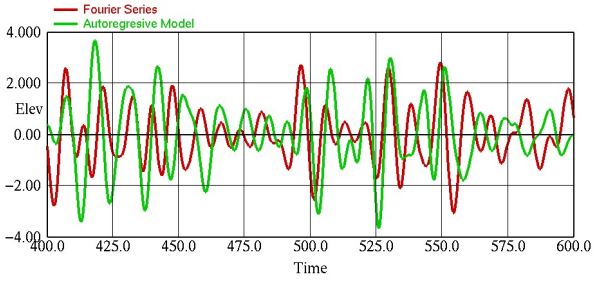

Fig. 3 Elevation for corresponding Fourier and ARM Waves

General Multi-dimensional Scalar Field

More recently, the ARMA approach has been extended to any random scalar field (Boukhanovsky & Degtyarev, 1995, 1996; Degtyarev & Boukhanovsky, 2000; Boukhanovsky, *et al.*, 2001). The general discrete vector autoregressive process takes the form:

$$\zeta_{\vec{V}} = \sum_{\vec{j}=\vec{0}}^{\vec{N}} \Phi_{\vec{j}} \zeta_{\vec{V}-\vec{j}} + \sigma_\varepsilon^2 \varepsilon_{\vec{V}}, \tag{9}$$

where the arrow over the corresponding index indicates multiple components of a scalar random process. $\vec{N}$ will define the regression order in each of the scalars and the total number of coefficients will be the product of the regression order ΠN_i, though the coefficient $\Phi_{\vec{0}}$ is 0.0 by definition. In general, a component can act as any scalar quantity such as temperature, salinity, or concentration of any substance.

To obtain the Yule-Walker equations for a scalar random field, multiply both sides of the multidimensional analog of (5) by $\zeta(\vec{u})$ and average both sides. This

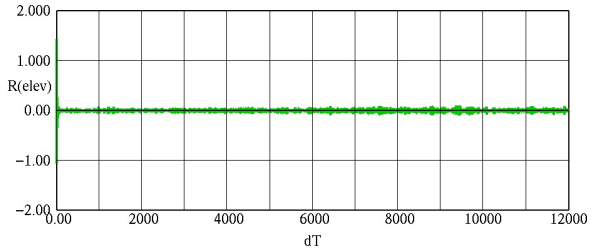

Fig. 4 Auto-covariance for Elevations from Autoregressive wave model

yields the generalized Yule-Walker equations:

$$K_\zeta(\vec{\tau}) = \sum_{\vec{j}=\vec{0}}^{\vec{N}} \Phi_{\vec{j}} K_\zeta(\vec{\tau} - \vec{\Delta} \circ \vec{j}); \quad \Phi_{\vec{0}} \equiv 0$$
$$\vec{\tau} S = \vec{v} - \vec{u}; \quad \vec{\Delta} \circ \vec{j} = \{\Delta_i \cdot j_i\}_{i=1}^{N}, \qquad (10)$$

where K_ζ is a multi-dimensional covariance, which is obtained as for the one dimensional problem ($K_\zeta(j \cdot \Delta t) = 1/(N_t - j)\sum_i^{N_t - j} \zeta(i+j)\zeta(i)$) but with $\vec{\tau}$ covering the matrix of increments in all dimensions. The variance of the white noise, σ_ε^2 can be determined from the system of equations (10) with $u = v$:

$$\sigma_\varepsilon^2 = V_\zeta - \sum_{\vec{j}=\vec{0}}^{\vec{N}} \Phi_{\vec{j}} K_\zeta(\vec{j} \cdot \vec{\Delta}). \qquad (11)$$

Some publications have noted an excessive sensitivity of the one-dimensional autoregressive model to noise in the raw data. One approach to mitigate this sensitivity is to use an over-determined generalized Yule-Walker system, solved using the method of least squares. In this case, the zero time autoregressive spectrum may not coincide with the variance of the simulated field, so the variance of white noise must be calculated using the spectral ratio to model the multivariate autoregressive variance:

$$\sigma_\varepsilon^2 = \frac{\pi^N K_\zeta(\vec{0})}{J} \qquad (12)$$
$$J = \int_0^{\pi/\Delta_1} \cdots (N) \cdots \int_0^{\pi/\Delta_N} \times \frac{\prod_{k=1}^{N} \Delta_k \, d\omega_k}{\left| \sum_{\vec{j}=\vec{0}}^{\vec{N}} \Phi_j \exp\left[i \sum_{k=1}^{N} (j_k \Delta_k \omega_k) \right] - 1 \right|^2}.$$

3-D Wave Model

For the application to numerical simulation, (9) is applied in three dimensions (2-D space + 1-D temporal) with $\vec{v}$ having have three components (x, y, t), resulting in the following expression for the wave elevation:

$$\zeta(x,y,t) = \sum_{ix=0}^{Nx} \sum_{iy=0}^{Ny} \sum_{it=0}^{Nt} \Phi_{(ix,iy,it)} \times \zeta(x - ix \cdot \Delta x, y - iy \cdot \Delta y, t - it \cdot \Delta t) + \sigma_\varepsilon^2 \varepsilon_{(ix,iy,it)}. \qquad (13)$$

Degtyarev & Boukhanovsky (2000) present numerical procedures for estimating the parameters of the 3-D ARM for waves and the dispersion of the corresponding field of white noise; as well as the transition to a wave field with an arbitrary distribution. The procedures generally follow the one-dimensional implementation and are based on the solution of the generalized Yule-Walker equations (10) though with additional computational features. It is these procedures which are being adapted for the present implementation.

IMPLEMENTATION OF THE AUTOREGRESSIVE WAVE MODEL IN A SIMULATION CODE

A principal objective of the current effort is to apply the autoregressive incident wave model to time domain ship motion simulations. An ARM is being implemented in the LAMP (Large Amplitude Motion Program) code, but the issues and procedures are substantially relevant to any hydrodynamic code and, to a large degree, the use of autoregressive ocean wave models in general.

LAMP is a so-called hybrid code that incorporates a 3-D body-nonlinear model of the Froude-Krylov and hydrostatic forces, a 3-D potential flow panel solution of the wave-body hydrodynamic disturbance forces, and a variety of time-domain models for the forces due to viscous roll damping, appendages such as rudders and bilge keels, propulsors, green-water-on-deck, and other effects. LAMP is a time-domain code, updating the disturbance flow field, computing hydrodynamic and non-hydrodynamic forces, and integrating motions and loads at each time step. In the calculation, the following incident wave quantities must be computed:

- Incident wave elevation at points on the hull surface in order to determine the incident wave waterline and create a panel model of the wetted hull surface
- Incident wave velocity ($\nabla\Phi_0$) at the control point of each body panel for the potential flow body boundary condition
- Incident wave pressure ($\rho\partial\Phi_0/\partial t$) on each wetted hull panel to calculate Froude-Krylov forces
- Incident wave velocity ($\nabla\Phi_0$) for the inflow to external forces models such as for appendage lift and drag.

In calculations using the standard Longuet-Higgins model, the incident wave is defined by a discrete set of component waves, each with a specified frequency, amplitude, heading, and phase, and these incident wave quantities are generally computed directly using Fourier-series expressions.

With the autoregressive wave model, the incident wave is defined by a regression order (N_x, N_y, N_z) and increment ($\Delta x, \Delta y, \Delta z$), a set of regression coefficients ($\Phi_{(ix,iy,it)}$), the corresponding variance of white noise (σ_ε^2) and a set of seeds for the pseudo-random number generator. At each time step of the simulation, the incident wave model is set up by the following steps:

1. Compute the elevation field on a grid of points around the ship
2. Estimate derivatives of the elevation in time and space
3. Solve for the velocity potential field beneath this elevation grid
4. Estimate derivatives of the velocity potential in time (Froude-Krylov pressure) and space (incident wave velocity)
5. Set up interpolation functions for the elevation and potential derivatives on the local grids.

The required evaluations of the incident wave elevation, velocity, and pressure are then handled by the interpolation functions. These steps are described in more detail below.

INCIDENT WAVE ELEVATION FIELD

The form of the expression for the autoregression wave elevation (13) naturally leads to the evaluation of the local wave elevation field on a grid of points with spatial increments corresponding to the Δx and Δy of the regression model:

$$\begin{aligned} x_{i_x} &= x_0 + (i_x - 1)\Delta x; \quad i_x = 1, ..., M_x \\ y_{i_y} &= y_0 + (i_y - 1)\Delta y; \quad i_y = 1, ..., M_y \\ t_{i_t} &= t_0 + (i_t - 1)\Delta t; \quad i_t = 1, ..., M_t \end{aligned}$$

$$\begin{aligned} \zeta_{(i_x,i_y,i_t)} &= \zeta(x_{i_x}, y_{i_y}, t_{i_t}) \\ &= \sum_{j_x=0}^{N_x} \sum_{j_y=0}^{N_y} \sum_{j_t=0}^{N_t} \Phi_{(j_x,j_y,j_t)} \\ &\quad \times \zeta_{(i_x-j_x,i_y-j_y,i_t-j_t)} + \sigma_\varepsilon^2 \varepsilon_{(i_x,i_y,i_t)} \end{aligned} \tag{14}$$

M_x and M_y define the size of the wave elevation evaluation grid, which is dictated by the size of the domain over which elevations are required and will generally be larger, sometimes far larger, than the length of the regression.

This elevation calculation is advanced in time along with the simulation itself. In the present application of the autoregressive wave model, the time step of the simulation is matched to the time step of the wave autoregression function. In principle, however, different time steps could be accommodated by either interpolating the wave elevation data in time or performing multiple wave time steps for each simulation time step.

Since the elevation at each point is dependent only on the elevations at lower or equal x, y, or t, it is explicit and easily calculated by sweeping through the elevation grid in X and Y at each time step. Calculating the elevation on a finite grid presents no major problem—the summation is simply truncated at the edge of the grid. This does result in a "ramp-up" area along the minimum x and y edges of the grid. Figure 5 shows an elevation plot of a relatively long-crested wave with regression order $10 \times 10 \times 10$, evaluated over a 64×64 grid. The ramp up area, whose width is roughly the regression order, can be seen near the edges.

In the present calculations, all elevations are initially set to 0, so there is a ramp-up in time as well. Figure 6 shows the minimum, maximum, and variance of the elevation across the grid over 1000 evaluations of the same autoregressive wave model. A ramp-up time of 20 to 25 evaluations (2 to 2.5 times the regression order in time) is evident. In most time-domain numerical simulations, including the present ones, this ramp-up can simply be retained in order to mitigate initial transients in the response. If, however, a fully developed wave is required from the start, the wave model can simply be evolved for the requisite number of cycles before starting the simulation. An alternative approach would be to initialize the wave field using a Fourier series or other explicit form.

The required extent of the wave elevation grid will generally be the region over which incident wave data is required plus some allowance at the minimum x and y edges for the "ramp-up" region described above. For the 3-D potential flow calculated using the present implementation, this is simply the extent of the hull's wetted surface. The issue is bit more complicated for simulations with forward speed or a significant amount of drift. The 3-D autoregressive wave model is generally cast in a global coordinate system, so the x and y grid lines of the evaluation must inherently be fixed in space. However, constructing a grid covering the entire range of the simulation would be impractical for a simulation of any length, so a local grid scheme has been implemented.

In the local grid scheme, the grid is moved with the ship but the grid lines are maintained at integer multiples of the grid increment. In effect, grid lines are added in front of the ship and removed from behind it as the simulation progresses. The addition of grid lines forward of the ship must account for the "ramp-up" time of these added lines. The resulting grid will therefore be considerably elongated in the direction of travel. For a typical seakeeping problem with a more-or-less constant speed and heading, the x extent of the grid will be:

$$x_0 = \left(\left\lfloor \frac{(x_g(t) - L/2)}{\Delta x} \right\rfloor - N_x \right) \Delta x \tag{15}$$

$$M_x = N_x + \left(\frac{L + 2UN_t\Delta t}{\Delta x} \right), \tag{16}$$

where $x_g(t)$ is the global x coordinate of the ship's center (mid-ships) at a given time, L is the ship length, N_x and

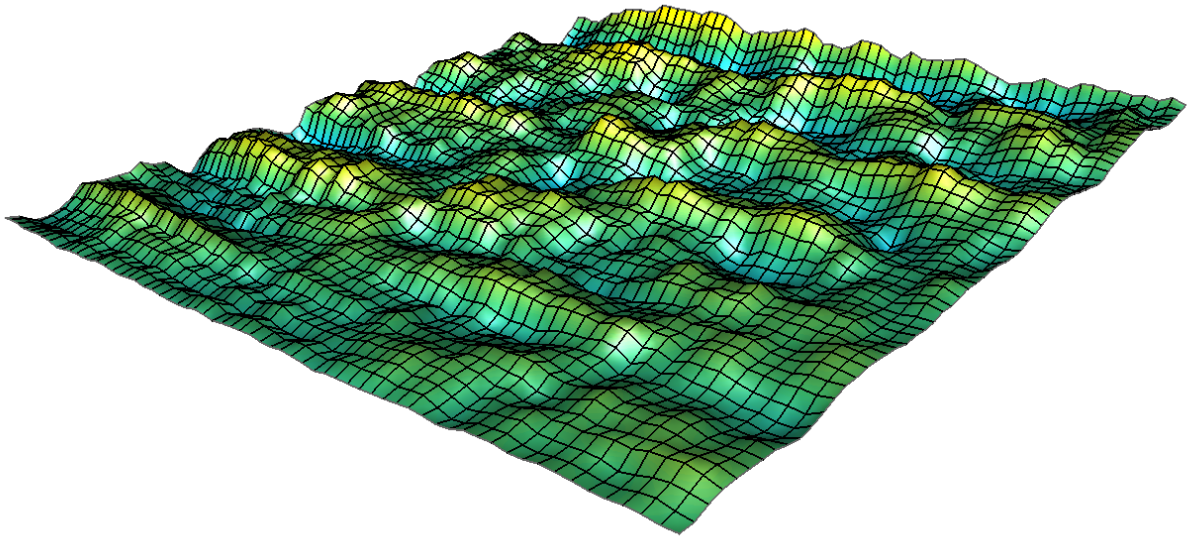

Fig. 5 Sample 3-D Elevation Field

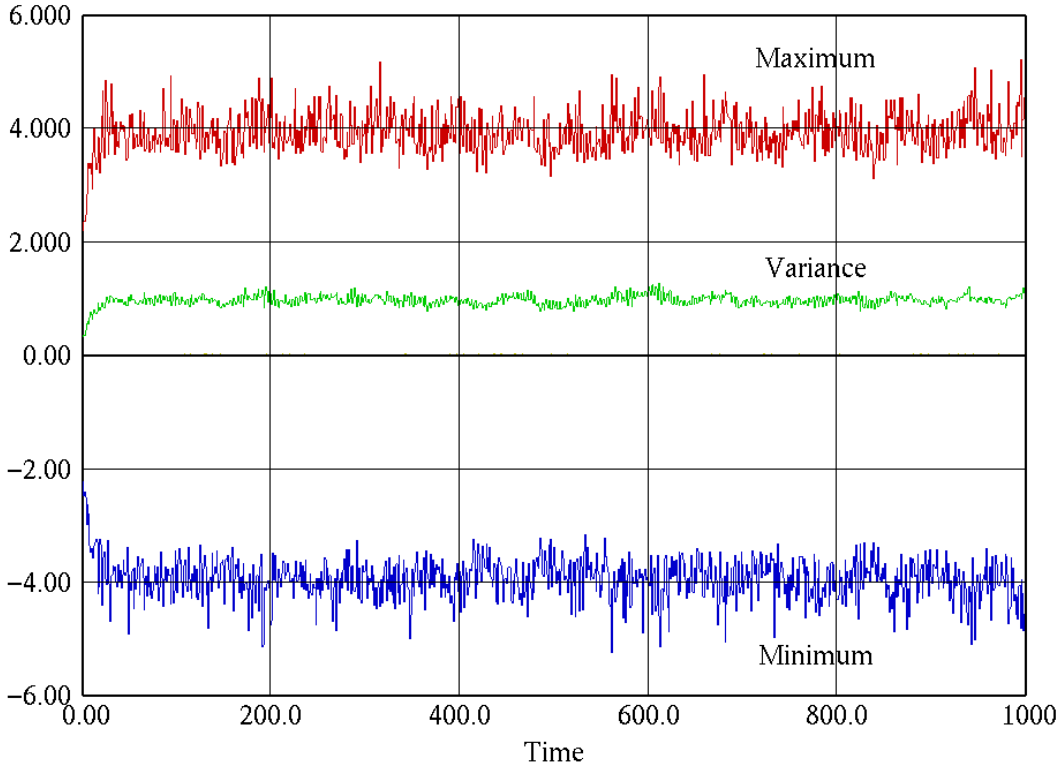

Fig. 6 Elevation Min, Max, and Variance *wrt* Time

Δx are the regression order and increment in x, N_t and Δt are the regression order and increment in time, and U is the ship speed. $\lfloor \bullet \rfloor$ is the integer floor function, used to round the grid extents to integer multiples of the grid spacing, so grid lines will be coincident from time step to time step.

For cases with large unsteady motion, including maneuvering in waves and broaching, the grid expansion must consider unsteady speed in both x and y. Figure 7 shows a notional wave evaluation grid (not every grid line is shown) at three simulation time steps for a ship in a slow speed turn.

Random White Noise

The term $\sigma_\varepsilon^2 \varepsilon_{(ix,iy,it)}$ in Equation (13) represents a field of white noise. σ_ε^2 is the variance of the white noise model and is a scalar value calculated from the regression coefficients as described above. Along with the regression coefficients, this value will be constant for stationary waves and a function of time for non-stationary (e.g. rising or falling) seas. $\varepsilon_{(ix,iy,it)}$ is a random function that should have unit variance and the same distribution as the wave elevations. For a Gaussian (normal) distribution, it can be readily approximated by the expression:

$$\varepsilon = \sum_{i=1}^{12} R_i - 6 \tag{17}$$

where R_i is a random value of uniform distribution and range [0,1], which is the typical value of the intrinsic pseudo-random number function available in most math libraries.

Repeatability of the Wave Model

In the same way that the "random" phases of the wave components provide different realizations of the irregular wave field in a Longuet-Higgins model, the "randomness" of $\varepsilon_{(ix,iy,it)}$ provides independent realizations of the ARM wave field. It is therefore necessary to be able to generate independent sets of these random values.

It is also highly desirable to be able to reproduce the identical calculation of the wave field. This is useful for visualizing the motion in waves, post-processing calculations such as relative motion and slamming, or simply repeating a simulation for a specific set of waves. To do this, it is necessary to use a pseudo-random number generator with a seed specification option and to record the seed as well as the size and origin of the regression grid.

An alternate to this approach would be to store elevation data as it is calculated, but the amount of data makes this impractical for most cases.

Derivatives of the Elevation Field

Derivatives of the wave elevation in space and time are not needed for the LAMP calculation itself, but are needed for calculation of the velocity potential field as described below. In the initial implementation, these derivatives are computed using finite difference of the values on the wave elevation grid. In order to allow a central difference calculation of the time derivative, the elevation calculation is run one time step ahead of the simulation. As the implementation of autoregressive continues, the calculation of these derivatives must be evaluated along with the effect and requirements of grid resolution and time step.

CALCULATION OF THE INCIDENT WAVE POTENTIAL FIELD

A significant challenge of using the ARM to generate ocean waves for numerical simulations is that the ARM provides only the elevation field, while numerical codes generally require the velocity and pressure fields beneath these waves. In boundary element methods (BEM) methods like LAMP, the pressure field is required in order to evaluate the Froude-Krylov forces and the velocity field is required to set up the body boundary condition of the disturbance potential. In order to address this challenge, the present implementation incorporates an "inverse problem" solver which computes the incident wave velocity potential ($\Phi_0(x,y,t)$) beneath the specified wave surface. This inverse problem solution, which is described in more detail in Gankevich & Degtyarev (2015), is summarized below.

The inviscid, incompressible potential flow beneath a free surface is described by the system of equations:

$$\begin{gathered} \nabla^2 \phi = 0 \\ \phi_t + \frac{1}{2}|\vec{\nabla}\phi|^2 + g\zeta = -\frac{p}{\rho} \quad \text{on } z = \zeta(x,y,t) \\ \frac{D\zeta}{Dt} = \vec{\nabla}\phi \cdot \vec{n} \quad \text{on } z = \zeta(x,y,t), \end{gathered} \tag{18}$$

where ϕ is the incident wave potential, D/Dt is the substantial derivative and $\vec{n}$ is the local normal vector to the free surface. The first of these equations satisfies continuity throughout the fluid domain while the second and third are dynamic and kinematic boundary conditions which are satisfied on the exact free surface, which, in this inverse problem, is known.

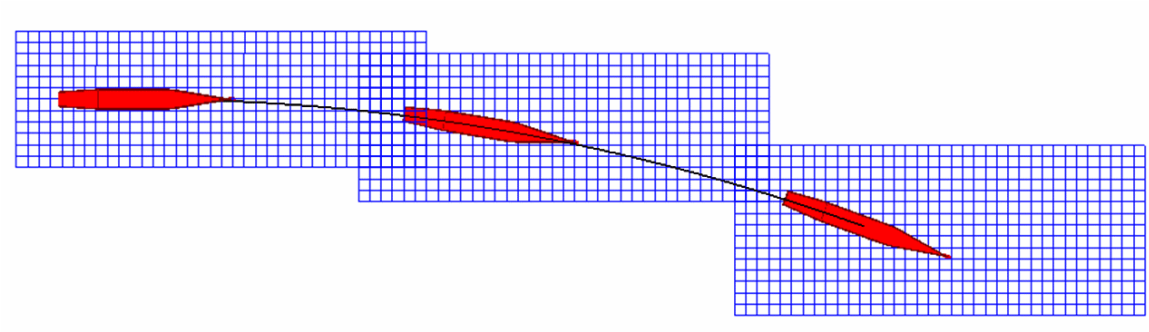

Fig. 7 Moving Elevation Grid for a Low Speed Turn

2-D Solution

For unsteady, two-dimensional (x,z,t) flow, (18) can be rewritten as:

$$\begin{aligned} &\phi_{xx}+\phi_{yy}=0 \\ &\phi_t+\frac{1}{2}(\phi_x^2+\phi_z^2)+g\zeta=-\frac{p}{\rho} \quad \text{on } z=\zeta(x,y,t) \\ &\zeta_t+\zeta_x\phi_x=\frac{\zeta_x}{\sqrt{1+\zeta_x^2}}\phi_x+\phi_z \quad \text{on } z=\zeta(x,y,t) \end{aligned} \tag{19}$$

The 2-D potential at any time can be written as the Fourier transform of a function multiplied by an exponential:

$$\phi(x,z)=\int_{-\infty}^{\infty}E(\lambda)e^{\lambda(z+ix)}d\lambda \tag{20}$$

This potential implicitly satisfies the continuity equation and can be substituted into the kinematic boundary condition in order to give:

$$\frac{\zeta_t}{1-i\zeta_x-i\zeta_x/\sqrt{1+\zeta_x^2}}=\int_{-\infty}^{\infty}\lambda E(\lambda)e^{\lambda(\zeta+ix)}d\lambda. \tag{21}$$

This expression represents a forward bilateral Laplace transform and can be inverted to yield a formula for the function $E(\lambda)$:

$$\begin{aligned} E(\lambda)=\frac{1}{2\pi i}\frac{1}{\lambda}\int_{-\infty}^{\infty}&\frac{\zeta_t}{1-i\zeta_x-i\zeta_x/\sqrt{1+\zeta_x^2}} \\ &\times e^{-\lambda(\zeta+ix)}dx. \end{aligned} \tag{22}$$

Substituting (22) into (20) yields the final result:

$$\begin{aligned} \phi(x,z)=&\frac{1}{2\pi i}\int_{-\infty}^{\infty}\frac{1}{\lambda} \\ &\left(\int_{-\infty}^{\infty}\frac{\zeta_t}{1-i\zeta_{x'}-i\zeta_{x'}/\sqrt{1+\zeta_{x'}^2}}e^{-\lambda(\zeta+ix')}dx'\right) \\ &\times e^{\lambda(z+ix)}d\lambda. \end{aligned} \tag{23}$$

It should be noted that while the free surface must be single valued, the slope of the wave is not assumed to be small, as has been assumed in previous solutions of the inverse problem. Gankevich & Degtyarev (2015) provide a comparison of the previous and present methods.

In the numerical implementation of this scheme for the elevations generated via the autoregressive model, the infinite upper and lower limits of the inner and outer integrals of (23) are replaced by the corresponding wave surface size (x_0, x_1) and wave number interval (λ_0, λ_1) so that the inner integral converges.

3-D Solution

Special Transform

The three-dimensional inverse potential problem for $\phi(x,y,z)$ can be solved with help of a special inversion formula which serves as a modified version of the Fourier transform:

$$F(x,y)=\iint_{-\infty}^{\infty}f(\lambda,\gamma)e^{i(\lambda x+\gamma y)+\zeta(x,y)\sqrt{\lambda^2+\gamma^2}}d\lambda d\gamma. \tag{24}$$

In order to derive the inversion formula, this expression is reduced to a two-dimensional convolution. To do this, the formula is rewritten in polar coordinates for both physical and wave number space:

$$F(\rho,\psi)=\int_0^{\infty}\int_0^{2\pi}rf(r,\theta)e^{ir\rho\cos(\psi-\theta)+r\zeta(\rho,\psi)}d\theta dr \tag{25}$$

where

$$\begin{aligned} &\lambda=r\cos\theta; \quad \gamma=r\sin\theta; \\ &x=\rho\cos\psi; \quad y=\rho\sin\psi. \end{aligned} \tag{26}$$

The following additional transformation is then applied to the radius values and ζ:

$$r=e^{r'}; \quad \rho=e^{-\rho'}; \quad \zeta=e^{-\rho'}\zeta'. \tag{27}$$

These substitutions result in a convolution integral

$$F(\rho',\psi) = e^{2r'} f(r',\theta) e^{(ie^{-\rho'}\cos\psi + e^{-\rho'}\zeta'(\rho',\psi))}. \quad (28)$$

Since convolution theory permits any converging integral transform to be applied to a convolution, a modified polar version of the Fourier transform is used:

$$\begin{aligned}\mathscr{F}'\{g(r,\theta)\}(r_1,\theta_1) = \int_0^{\infty}\int_0^{2\pi} -e^{-2r} g(r,\theta) \\ \times e^{-ie^r r_1 \cos(\theta_1-\theta)} d\theta\, dr.\end{aligned} \quad (29)$$

Applying this transform to both sides of (28) yields the final formula:

$$\mathscr{F}\{F(x,y)\} = \mathscr{F}\left\{\frac{f(x,y)}{x^2+y^2}\right\} \mathscr{F}\{e^{ix+\zeta(x,y)}\}. \quad (30)$$

This formula has two principle uses in the solution of the three-dimensional inverse potential problem. First, it allows the inversion of the initial modified Fourier transform (24). Second, it can be used to compute $F(x,y)$ efficiently using fast Fourier transforms (FFTs).

Formula Derivation

The formula for the 3-D problem is derived in much the same way as in the 2-D problem, but using the special transform described above rather than the bilateral Laplace transform, and normalizing horizontal coordinates to provide a dimensionless form of the convolution.

Considering a square region with side N over which the inverse problem is to be solved, the coordinate transform $(x,y) \to (xN, yN)$ is used to rewrite (18) with dimensionless x and y:

$$\begin{gathered}\frac{\phi_{xx}}{N^2} + \frac{\phi_{yy}}{N^2} + \phi_{zz} = 0 \\ \phi_t + \frac{1}{2}\left(\frac{\phi_x^2}{N^2} + \frac{\phi_y^2}{N^2} + \phi_z^2\right) + g\zeta = -\frac{p}{\rho} \\ \text{on } z = \zeta(x,y,t) \\ \zeta_t + \frac{\zeta_x}{N^2}\phi_x + \frac{\zeta_y}{N^2}\phi_y = \frac{\zeta_x}{Nd}\phi_x + \frac{\zeta_y}{Nd}\phi_y + \phi_z \\ \text{on } z = \zeta(x,y,t)\end{gathered} \quad (31)$$

where $d = \sqrt{N^2 + \zeta_x^2 + \zeta_y^2}$.

The 3-D potential at any time can is defined as:

$$\phi(x,y,z) = \int_{-\infty}^{\infty}\int E(\lambda,\gamma) e^{M(iN(\lambda x+\gamma y)+z\sqrt{\lambda^2+\gamma^2})} d\lambda\, d\gamma. \quad (32)$$

Here λ and γ are dimensionless wave numbers generated by the transform $(\lambda,\gamma) \to (\lambda M, \gamma M)$. Substituting this expression into the kinematic boundary condition yields:

$$\begin{aligned}\zeta_t = \int_{-\infty}^{\infty}\int E(\lambda,\gamma) e^{M(iN(\lambda x+\gamma y)+z\sqrt{\lambda^2+\gamma^2})} \\ \times \frac{M}{Nd}\left[N^3\sqrt{\lambda^2+\gamma^2} - i\lambda\zeta_x(d-N)\right. \\ \left. - i\gamma\zeta_y(d-N)\right] d\lambda\, d\gamma.\end{aligned} \quad (33)$$

In order to obtain the convolution formula, the transformations (26) and (27) are applied:

$$\begin{aligned}\zeta_t = \int_{-\infty}^{\infty}\int_0^{2\pi} E(r',\theta)\frac{Me^{2r'}}{Nd'}\left[N^3\right. \\ - ie^{\rho'}\cos(\theta-\psi)\zeta_{\rho'}(d'-N) \\ \left. - ie^{\rho'}\sin(\theta-\psi)\zeta_{\psi'}(d'-N)\right] \\ \times e^{Me^{r'-\rho'}(iN\cos(\theta-\psi)+\zeta)} d\theta\, dr',\end{aligned} \quad (34)$$

where $d' = \sqrt{N^2 + e^{2\rho'}(\zeta_x^2 + \zeta_y^2)}$.

Finally, the modified Fourier transform (29) can be applied to both sides of this equation to derive the formula for the function E:

$$\begin{aligned}\mathscr{F}\{\zeta_t(x,y)\} = \mathscr{F}\left\{\frac{E(\lambda,\gamma)}{\lambda^2+\gamma^2}\right\} \\ \times \mathscr{F}\left\{f(x,y)e^{M(iNx+\zeta)}\right\}\end{aligned} \quad (35)$$

$$f(x,y) = M\frac{N^2 + i\zeta_x\left(\sqrt{N^2+\zeta_x^2+\zeta_y^2} - N\right)}{N\sqrt{N^2+\zeta_x^2+\zeta_y^2}} \quad (36)$$

Numerical Implementation

Formula (30) can now be used to derive the velocity potential (32) as one inverse and two forward Fourier transforms:

$$\phi(x,y,z) = \mathscr{F}^{-1}\left\{\mathscr{F}\left\{\frac{E(x,y)}{x^2+y^2}\right\}\mathscr{F}\left\{e^{M(iNz+\zeta)}\right\}\right\} \quad (37)$$

Formula (35) for the function E is used to obtain the final result:

$$\phi(x,y,z) = \mathscr{F}^{-1}\left\{\frac{\mathscr{F}\{\zeta_t(x,y)\}\mathscr{F}\{e^{M(iNx+z)}\}}{\mathscr{F}\{f(x,y)e^{M(iNx+\zeta)}\}}\right\} \quad (38)$$

This formula allows for a direct calculation of the incident wave velocity potential field from a distribution of wave elevation and its derivatives in space and time. The calculation has no dependency on time and

can be evaluated at each time step in a numerical simulation. If the elevation data is specified on a regular rectangular grid, as will be the case for elevations from the autoregressive model, the calculation can be performed very rapidly using FFTs. In the present implementation, the inverse potential calculation has been readily implemented using the FFTW library (`http://fftw.org`), which is freely available under the GNU General Public License.

Figure 8 shows a cross-section of the velocity potential field evaluated by this method on a $64 \times 64 \times 20$ grid beneath a regular wave. Figure 9 shows slices of the velocity potential field evaluated beneath a wave surface generated by the autoregressive wave model.

Estimate and Interpolation of Potential Derivatives

The inverse velocity potential calculation (38) provides the potential on the grid of (xy)-points corresponding to the elevation data produced by the ARM (or other method). There is no easy way to derive analogous formula for the derivatives of the velocity potential. However, numerical experiments suggest that derivatives calculated using finite difference techniques are adequate for ship hydrodynamics problems. The lateral (x,y) resolution will, of course, be dependent upon the resolution of the elevation data.

However, in the vertical, z, direction, formula (38) can be evaluated for any z, so the resolution and range of the vertical distribution of the potential and its derivatives can be selected based on the requirements of the problem.

In the present implementation, the velocity potential is computed at a series of z values from the free surface to the draft of the ship. Derivatives are then computed using finite differences. Spatial interpolation of these derivatives are then set up using Chebyshev polynomials, which can evaluated to provide the velocity or pressure at each body control point. A similar 2-D Chebyshev interpolation is set up for the elevations.

The resulting velocity and pressure field may have an advantage over the Fourier representations in that the derivatives are consistent with the resolution of the elevation and pressure while the Fourier velocities can be overly sensitive to high-frequency components.

SUMMARY AND STATUS

Degtyarev & Reed (2011, 2012) presented the development of an autoregression model for incident random waves that is far more computationally efficient than the Fourier series like models of St. Denis & Pearson, Rosenblatt, Sveshnikov, or Longuet-Higgins. This model is amenable to modeling the synoptic and temporal processes associated to the development and evolution of ocean waves in a storm.

Degtyarev & Reed also showed that the waves produced by the autoregression model have the correct statistical characteristics spatially and temporally to represent ocean waves—the desired wave spectra can be reproduced and the distributions of physical characteristics is correct. Although the model does not explicitly contain the physics of gravity waves, by using 2- and 3-dimensional (1- or 2-dimensions in space + time) autoregression functions based on actual wave measurements, the model even captures the dispersion relation for gravity waves.

The present work continues that development by implementing an autoregressive incident wave model in a time-domain numerical simulation code based on the body-nonlinear hydrostatic and Froude-Krylov forces and a 3-D potential flow solution of the wave-body hydrodynamic interaction problem. Several key aspects of this implementation are described, including the effective evaluation of the ARM on a set of moving grids for a simulation with steady or unsteady forward speed and the calculation of the incident wave velocity potential field beneath a prescribed wave surface. The latter procedure is not only a critical element of the application of the ARM, but provides a mechanism for implementing other non-traditional ocean wave models in numerical simulations.

At the time of writing of this paper, the numerical implementation of the autoregressive model for incident waves is not yet fully operational. As such, it is too early to be able to evaluate the practicality of using an ocean wave ARM for numerical seakeeping simulations in irregular waves. However, the potential for providing a very efficient seaway model for long-term simulations is evident.

It should be noted that the validation of the wave field and pressure generated by an ARM of ocean waves, and the predicted ship responses to those waves, presents a challenge. The ARM, with its integral randomness, can only be validated in a statistical sense. The most effective validation approaches for wave field models and ship motion predictions have generally been on the detailed comparison to specific experimental runs of some kind. The inability of the ARM to deterministically reproduce a measured wave history precludes such a side-by-side comparison.

Several areas where future research is needed have been identified. One of the most critical appears to be the derivation of a direct method for computing the velocities in the fluid domain, a method similar to that used to compute the velocity potential.

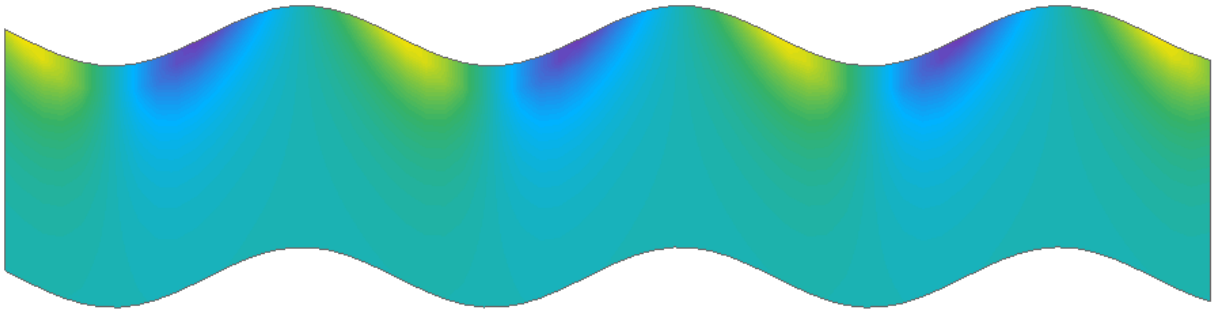

Fig. 8 3-D Potential for Regular Wave

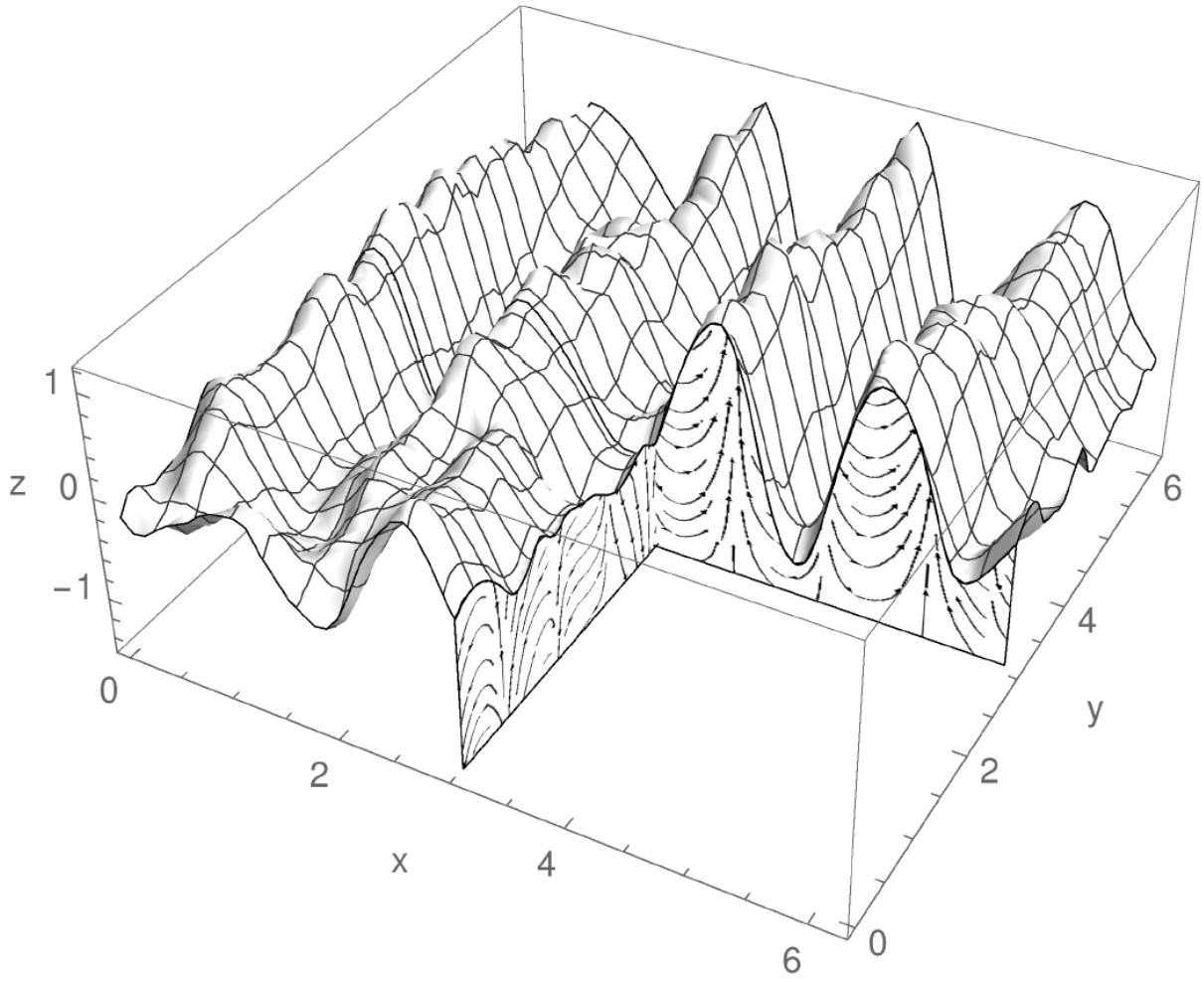

Fig. 9 3-D Potential for ARM Wave

ACKNOWLEDGMENTS

Professor Degtyarev's work with NSWCCD has been supported by the Office of Naval Research Global's Visiting Scientist Program. The authors are grateful to Dr. Woei-Min Lin of ONRG and Dr. Vadim Belenky of NSWCCD for their effort in arranging this effort.

REFERENCES

Beck, R. F. & A. M. Reed (2001) Modern Computational Methods for Ships in a Seaway. *Trans. SNAME*, Vol. 109, pp. 1–51.

Belenky, V. (2005) On Long Numerical Simulations at Extreme Seas. *Proc. 8th Int'l. Ship Stability Workshop*, Istanbul, Turkey, 7 p.

Boukhanovsky, A. & A. B. Degtyarev (1995) On the Estimation of the Motion Stability in Real Seas. *Proc. Int'l Symp. Ship Safety in a Seaway: Stability, Maneuverability, Nonlinear Approach*, Kaliningrad, Vol. 2, Paper 8, 10 p.

Boukhanovsky, A. V. & A. B. Degtyarev (1996) Probabilistic modelling of storm waves fields. *Proc. Int'l Conf. "Navy and Shipbuilding Nowadays"*, St. Petersburg, Vol. 2, A2–29, 10 p. (In Russian)

Boukhanovsky, A., V. Rozhkov & A. B. Degtyarev (2001) Peculiarities of Computer Simulation and Statistical Representation of Time-Spatial Metocean Fields. In: *Computational Science—ICCS*, LNCS 2073, Springer, Part I, pp. 463–472.

Box, G. E. P., G. M. Jenkins & G. C. Reinsel (2008) *Time series analysis: Forecasting and control*, 4th Ed., Wiley, xx+746 p.

Degtyarev, A. B. & A. Boukhanovsky (2000) Peculiarities of motion of ship with low buoyancy on asymmetrical random waves. *Proc. Int'l Conf. Stability of Ships and Floating Vessels*, Launceston, Tasmania, Australia, Vol. 2, pp. 665–679.

Degtyarev, A. B., & Reed, A. M. (2011) Modeling of Incident Waves Near the Ship's Hull: Application of Autoregressive Approach to Problems of Simulation in Rough Seas. *Proc. 12th Int'l. Ship Stability Workshop*, Washington, D.C., pp. 175-187.

Degtyarev, A. B. & Reed, A. M. (2012) Synoptic and Short-Term Modeling of Ocean Waves. *Proc. 29th Symp. Naval Hydromechanics*, Goteborg, Sweden, L. Larsson (ed.), 21 p. (Also: *Int'l. Shipbuilding Progress*, 2013, 60(1–4):523-553.)

Gankevich, I. & Degtyarev, A.B. (2015) Computation of Pressures in Inverse Problem in Hydrodynamics of Potential Flow. *Proc. 12th Int'l. Conf. Stability of Ships and Ocean Vehicles*, Glasgow, UK, 5 p.

Gurgenidze, A. T. & Y. A. Trapeznikov (1988) Probabilistic model of wind waves. In: *Theoretical foundations and methods of calculating wind waves*, Leningrad, Gidrometeoizdat, pp. 8–23.

Longuet-Higgins, M. S. (1962) The Statistical Analysis of a Random, Moving Surface. *Phil. Trans. Royal Soc. London*, Ser. A, Mathematical and Physical Sciences, 249(966):321–387.

Rozhkov, V. A. & Y. A. Trapeznikov (1990) *Probabilistic models of oceanographic processes*, Leningrad, Gidrometeoizdat.

Spanos, P. D. (1983) ARMA Algorithms for Ocean Wave Modeling. *J. Energy Resources Technology*, Trans. ASME, Vol. 105:300–309.